Two Autoimmune Diabetes Loci Influencing T Cell Apoptosis Control Susceptibility to Experimental Autoimmune Myocarditis[1]

Mehmet L. Guler,* Davinna L. Ligons,* Yan Wang,* Michael Bianco,* Karl W. Broman,† and Noel R. Rose[2]*‡

The pathogenesis of immune-mediated myocarditis depends on genetic and environmental factors. To study the genetic mechanisms, we have developed a model of experimental autoimmune myocarditis in the A.SW mouse. Here we provide evidence that loci on murine chromosome 6, and possibly chromosome 1, are involved in regulating susceptibility. Moreover, these loci overlap with loci implicated in other autoimmune diseases including diabetes in the NOD mouse. These two loci also regulate apoptosis in thymocytes as well as peripheral T cells in the NOD mouse, and we report further that A.SW mice demonstrate the same characteristics in apoptosis. These results suggest that common pathogenetic mechanisms involving apoptosis of both thymic and peripheral T cells are shared by multiple autoimmune diseases. *The Journal of Immunology,* **2005, 174: 2167–2173.**

Dilated cardiomyopathy accounts for 25% of cases of heart failure and is a primary cause of sudden death in adults <40 years of age (1, 2). Although the etiology of dilated cardiomyopathy is unknown, over 10% of cases are associated with a preceeding viral myocarditis—often induced by coxsackievirus B3 (CB3) [3] (3). Because heart failure generally occurs long after infection, and is relatively rare, a genetically determined autoimmune response has been implicated as its cause. Several lines of evidence, particularly from animal models, suggest that chronic myocarditis and dilated cardiomyopathy result from a progressive autoimmune response initiated by an earlier viral myocarditis (4). A disease resembling human myocarditis can be produced in mice using CB3 (5). All strains of mice develop an acute myocarditis characterized by active viral replication and a vigorous inflammatory response that resolves with clearance of viable virus. In a few strains of mice, however, especially A/J and other strains sharing the A background, a second phase of inflammation characterized by diffuse mononuclear infiltration occurs in the absence of infectious virus. Furthermore, production of anti-cardiomyocyte IgG autoantibodies can only be demonstrated in genetically susceptible strains (6–9). These observations support the hypothesis that initial infection with CB3 virus causes release and presentation of cardiac Ags in an inflamed immunogenic context, leading to stimulation of autoreactive lymphocytes in genetically susceptible mice. These heart-specific autoreactive lymphocytes subsequently induce autoimmune myocarditis and dilated cardiomyopathy long after acute viral myocarditis has cleared.

To further test the autoimmune hypothesis of CB3-induced myocarditis, we originated a virus-free, experimentally induced autoimmune myocarditis (EAM) in the mouse (10). In this model, susceptible strains immunized with purfied cardiac myosin in CFA develop chronic myocarditis characterized by a diffuse mononuclear infiltrate and cardiac specific autoantibodies. The cardiac lesions resemble the second (virus-independent) phase of CB3 virus-induced myocarditis. Autoreactive T cells derived from susceptible cardiac myosin-immunized mice can transfer disease to naive recipients after in vitro expansion (11, 12). Strains of mice resistant to the late phase of virus-induced myocarditis develop no cardiac pathology following immunization with cardiac myosin. Therefore, it is likely that mechanisms leading to genetic predisposition to autoimmune myocarditis are similar in both the virus-induced and Ag-induced experimental models, making EAM an effective tool in the study of the pathogenesis of virus-induced autoimmune disease (10).

Like other autoimmune diseases, the mechanisms leading to susceptibility to autoimmune myocarditis are certainly multifactorial and genetically complex. Defining the genetic factors underlying susceptibility will greatly enhance our understanding of autoimmune diseases and related immunopathologic processes. We reported previously that the MHC influences susceptibility to myocarditis (13). In an effort to identify other non-H-2 genetic loci that control susceptibility to CB3 virus-induced autoimmune myocarditis, our laboratory initially compared inheritance of the susceptibility trait in AxB and BxA recombinant inbred strains ($n = 13$ and $n = 9$, respectively; Ref. 14). With all of the available genomic markers at the time, suggestive linkage to the TCR-α locus on murine chromosome (Chr.) 14 was tentatively identified. Current analysis, with the addition of more markers based on single-strand-length polymorphic (SSLP) markers, has led us to conclude that these original observations were probably false positives and require analysis of many more meiotic combinations, beyond the limited number of meiotic combinations that are represented by

*Department of Pathology, The Johns Hopkins University, Baltimore, MD 21205; and †Department of Biostatistics and ‡Feinstone Department of Molecular Microbiology and Immunology, The Johns Hopkins University, Bloomberg School of Public Health, Baltimore, MD 21205

Received for publication August 16, 2004. Accepted for publication November 11, 2004.

The costs of publication of this article were defrayed in part by the payment of page charges. This article must therefore be hereby marked *advertisement* in accordance with 18 U.S.C. Section 1734 solely to indicate this fact.

[1] The authors' research is supported by National Institutes of Health Research Grants R01 HL67290, R01 HL 70729, R21 A151835, and R01 HL077611 and a grant from the MARRC. M.G. is supported by National Institutes of Health Training Grant AI07-247

[2] Address correspondence and reprint requests to Dr. Noel R. Rose, Department of Pathology, The Johns Hopkins University, 720 Rutland Avenue, Baltimore, MD 21205. E-mail address: nrrose@jhsph.edu

[3] Abbreviations used in this paper: CB3, coxsackievirus B3; Chr., chromosome; Dxm, dexamethasone; Cy, cyclophosphamide; EAM, experimental autoimmune myocarditis; LOD, logarithm of the odds; SSLP, single strand length polymorphic; QTL, quantitative trait linkage.

0022-1767/05/$02.00

recombinant inbred strains. In a fresh approach, we decided to identify non-H-2 loci controlling differential susceptibility to experimentally induced (myosin/CFA-induced) autoimmune myocarditis in the A.SW and B10.S strains, which are identical at H-2 (H-2^s). The induced model of autoimmune myocarditis demonstrates less variability in phenotype, perhaps due to diminished influence of infection, thereby facilitating the isolation of additional susceptibility loci in this genetically complex disease.

Materials and Methods

Mice

The H-2^s congenic mice A.SW and B10.S, as well as NOD mice were purchased from The Jackson Laboratory and were bred and maintained in the conventional housing facilities at The Johns Hopkins University (Baltimore, MD). F_1 mice were generated through a male A.SW $\times$ female B10.S cross. F_2 animals were generated through an $F_1 \times F_1$ intercross.

EAM: induction and phenotype quantification

EAM was induced in male and female, 8- to 10-wk-old, A.SW, B10.S, F_1 and F_2 mice by two axillary s.c. injections of 200 and 250 μg of purified murine cardiac myosin in PBS emulsified (1:1 ratio) in CFA (Sigma-Aldrich), in a total volume of 100 μl, on days 0 and 7, respectively. On day 0, mice also received an i.p. injection of 500 ng of pertussis toxin (Sigma-Aldrich) in 100 μl of PBS to increase adjuvanticity. The myosin was prepared from an equal mixture of A.SW and B10.S hearts and has been described in detail before (10, 15). CFA was additionally supplemented with 100 ng of H37Ra extract (Difco). After 21 days, hearts were isolated, bisected coronally, and fixed in 10% formaldehyde. The hearts were examined grossly for lesions and were bisected along any major lesions that were identified. Coronal sections allowed visualization of all four chambers of the heart and intraventricular septum. The hearts were then sent to Associated Tissue Technologies where they were embedded in paraffin, and five coronal sections (5 μM thick each) at different levels throughout the heart were cut and stained with H&E according to standard protocol. The presence of myocarditis was assessed by examining the hearts histologically using a light microscope fitted with a digital camera (Olympus, magnafire 2.1). The degree of myocarditis was quantified by measuring the percent area of myocardium infiltrated by chronic inflammatory cells in the most affected section using image analysis software from Scion Corporation (⟨www.scioncorp.com⟩). Digital photos of entire heart sections were obtained using a 4$\times$ objective. The area of infiltrated myocardium was manually outlined using the image analysis software and compared with the outlined area of the entire heart. Most hearts were assessed at least two times on separate occasions to determine intrameasurement variability which was no more than 6%.

Genotype analysis

Genomic DNA was prepared from tail tissue as described previously (16). Genomic analysis was performed on all F_2 mice through determination of the inheritance pattern of A.SW and B10.S alleles of SSLP markers distributed throughout the murine genome. Eighty-one SSLP markers at ~20 cM intervals throughout the murine genome, listed to be polymorphic between the parental strains (A/J and C57BL/6) in the MIT genome center database (⟨http://www-genome.wi.mit.edu/⟩), were confirmed to be polymorphic between A.SW and B10.S (see Table I for a list of markers). PCR primers were generated for each SSLP marker and genomic DNA from each F_2 individual was amplified in a PCR with the following conditions: a 20-μl total reaction volume contained 80 ng of genomic DNA, 1$\times$ PCR buffer as supplied by manufacturer (Invitrogen Life Technologies), 4 nmol of dNTPs, 50 nmol of $MgCl_2$, 7.92 pmol of each primer, and 0.8 U of *Taq* polymerase (Invitrogen Life Technologies). Amplification was achieved through the following thermal cycler conditions: 1 time at 95°C for 2 min; 38 times at 94°C for 45 s, 54°C for 45 s, and 72°C for 30 s; and 1 time at 72°C for 7 min. PCR products were analyzed by gel electrophoresis on 2.5% high resolution agarose (Metaphore Agarose; Biowhittaker) containing ethidium bromide.

Statistical analysis for genetic linkage

All statistical analyses were performed with R/qtl version 0.97-22 (17), an add-on package to the statistical software, R (18). Our initial analysis was based on genome-wide genotype data from 144 individuals with extreme phenotypes (percent myocarditis <4.5 or $>26.5\%$). For this analysis, the phenotype was treated as dichotomous, and linkage analysis was performed using the method of Xu and Atchley (19). Statistical significance was

Table I. *SSLP markers used in this study*

Marker	Position (cM)	A.SW (bp)	B10.S (bp)
D1Mit231	8.7	219	267
D1Mit373	14.2	138	124
D1Mit278	17.5	222	210
D1Mit213	25.1	96	108
D1Mit435	37.2	90	102
D1Mit334	49.2	90	98
D1Mit26	64.5	216	194
D1Mit15	86.3	186	160
D1Mit407	103.8	134	120
D2Mit416	12	116	124
D2Mit370	27.3	104	121
D2Mit66	48.1	278	256
D2Mit423	68.9	164	148
D2Mit113	87.4	128	148
D3Mit367	9.7	158	146
D3Mit209	25.1	262	244
D3Mit315	40.4	90	100
D3Mit293	59	92	104
D4Mit211	10.9	153	145
D4Mit81	31.7	204	160
D4Mit116	36.1	152	136
D4Mit359	41.4	130	118
D4Mit146	52.5	149	125
D4Mit338	54.6	122	100
D4Mit249	57.9	210	224
D4Mit203	60.1	144	118
D4Mit251	66.7	106	116
D4Mit310	71	127	117
D5Mit348	5.5	133	123
D5Mit255	25.1	132	120
D5Mit366	44.8	141	175
D5Mit31	66.7	238	210
D5Mit409	77.6	214	198
D6Mit312	9.8	124	110
D6Mit226	29.5	170	150
D6Mit36	40.4	178	196
D6Mit287	44.8	150	88
D6Mit219	51.4	178	188
D6Mit339	54.6	110	118
D6Mit294	63.4	132	126
D6Mit373	66.7	120	106
D6Mit15	65.6	195	260
D7Mit267	10.9	182	196
D7Mit90	28.4	280	260
D7Mit164	45.9	331	309
D7Mit259	67.8	152	148
D8Mit94	10.9	130	156
D8Mit69	32.8	156	144
D8Mit364	68.9	212	200
D9Mit67	13.1	136	124
D9Mit47	33.9	206	196
D9Mit12	53.6	82	93
D9Mit321	69.6	179	201
D10Mit83	4.4	275	251
D10Mit214	15.3	132	126
D10Mit274	38.68	160	140
D10Mit134	57.9	125	101
D10Mit237	72.1	96	87
D11Mit82	10.9	148	164
D11Mit242	31.7	138	122
D11Mit288	53.6	110	126
D11Mit253	75.4	95	81
D12Mit124	9.8	124	144
D12Mit14	31.7	146	130
D12Mit280	51.4	144	126
D13Mit275	7.7	118	108
D13Mit99	25.1	177	203
D13Mit213	40.4	160	148
D13Mit77	53.6	320	280
D14Mit98	3.3	164	152
D14Mit14	16.4	248	270
D14MIT101	26.2	117	133

(*Table continues*)

Table I. (*Continued*)

Marker	Position (cM)	A.SW (bp)	B10.S (bp)
D14Mit34	47	138	158
D14Mit266	67.8	176	148
D15Mit267	10.9	312	296
D15Mit270	27.3	188	200
D15Mit239	36.1	100	112
D15Mit245	56.8	101	119
D16Mit87	7.7	124	137
D16Mit59	25.1	189	175
D16Mit178	40.4	137	127
D17Mit20	29.5	170	180
D17Mit2	43.7	220	230
D18Mit158	9.8	266	276
D18Mit40	25.1	132	142
D18Mit4	37.2	188	210
D19Mit61	9.8	149	131
D19Mit46	24	133	115
D19Mit70	38.3	225	196
D19Mit137	55.7	132	122
DXMit140	20.8	122	108
DXMit172	40.4	134	148
DXMit186	57.9	120	128

determined by a permutation test, using 1000 permutation replicates (20). The analysis was also performed considering the female and male F_2 mice separately.

Analysis of the quantitative phenotype for all individuals was performed using the multiple imputation approach of Sen and Churchill (21). The null distribution of the logarithm of the odds (LOD) score calculated by the multiple imputation approach was seen to vary according to proportion of genotype information available for a region, and so we derived chromosome-specific LOD thresholds and p values, though still making proper adjustment for the genome-wide scan. Let P_c denote the chromosome-specific p value for chromosome c, estimated via a permutation test; that is, P_c is the proportion of the permutations for which the maximum LOD score on chromosome c was greater than the maximum LOD score on that chromosome in the observed data. We obtain a genome-scan-adjusted p value as $P'_c = 1 - (1 - P_c)^{L/L_c}$ where L_c is the genetic length of chromosome c and L is the total genetic length of the genome. As considerably greater precision is required for the chromosome-specific p values due to this adjustment, 100,000 permutation replicates were used.

Dexamethasone (Dxm)-induced thymocyte apoptosis

The method was adapted from Bergman et al. (22). Male and female 6- to 8-wk-old A.SW, B10.S, and NOD mice were each injected i.p. with 200 μg of Dxm (Sigma-Aldrich) dissolved in 300 μl of PBS. Untreated mice served as controls. Twelve hours later, mice were sacrificed and thymuses were collected. Single cell thymocyte suspensions were prepared by gently dispersing thymuses through 25-μm nylon-mesh filters. Apoptotic cells were then quantitated using the TUNEL reaction detailed below.

Cyclophosphamide (Cy)-induced peripheral lymphocyte apoptosis

The method was adapted from Colucci et al. (23). Male and female 6- to 8-wk-old A.SW and B10.S mice were each injected i.p with 7.5 mg of Cy (Sigma-Aldrich) dissolved in 300 μl of H_20. Untreated mice served as controls. Mice were sacrificed 16 h later, and inguinal, axial cervical, and mesenteric lymph nodes were collected. Single-cell suspensions were prepared by gently dispersing the lymph nodes over 25-μm nylon-mesh filters. Apoptotic cells were then quantitated using the TUNEL reaction detailed below.

Determination of apoptotic cells by TUNEL

Cells (from thymuses or lymph nodes prepared as above) were placed in 200 μl V-bottom 96-well plates, washed 3× with PBS, and fixed in 200 μl of 4% paraformaldehyde in PBS for 30 min at room temperature with gentle agitation. The cells were then washed once with PBS and permeablized in 200 μl of 0.1% saponin (Sigma-Aldrich) in PBS on ice for 3 min. After washing 2× with PBS, apoptotic cells were determined using the TUNEL reaction. We used the FITC In Situ Cell Death Detection kit from Roche Diagnostics and followed the manufacturer's protocols. Briefly, cells were incubated with 50 μl of TdT enzyme and FITC-conjugated dUTP for 1 h at 37°C. Finally, cells were washed three times with PBS, and analyzed by flow cytometry on a FACScan (BD Biosciences). No prior drug treatment, and exclusion of TdT from the TUNEL reaction were included as negative and specificity controls, respectively.

Statistical analysis of phenotypes

All means and SDs were derived with standard methods, and p values for two-tailed unpaired comparisons between two phenotypes (e.g., percentage of myocarditis in A.SW vs B10.S, or percentage of apoptosis in A.SW thymocytes vs B10.S thymocytes, etc.) were calculated using a standard Student t test.

Results

Susceptibility to EAM is a quantitative heritable trait

We had previously shown that A and C57BL/6 mouse strains differ in their susceptibility to CB3 virus-induced and cardiac myosin-induced autoimmune myocarditis (10, 13). We initially observed that this trait was influenced by the H-2 locus but that non-H-2 background genes play a dominant role (24, 25). To focus on non-H-2 loci, we fixed the H-2 locus and compared susceptibility to cardiac myosin-induced EAM in the H-2^s congenic strains A.SW and B10.S.

After two injections, a week apart, with murine cardiac myosin in CFA, together with a single administration of pertussis toxin during the first immunization, A.SW mice developed a dense myocardial infiltrate composed mostly of mononuclear cells and a few scattered neutrophils. B10.S mice, in contrast, developed minimal inflammation. Quantitation of this trait through measurement of percent area of myocardium involved by inflammation revealed highly significant differences in susceptibility (Fig. 1*A*). In A.SW

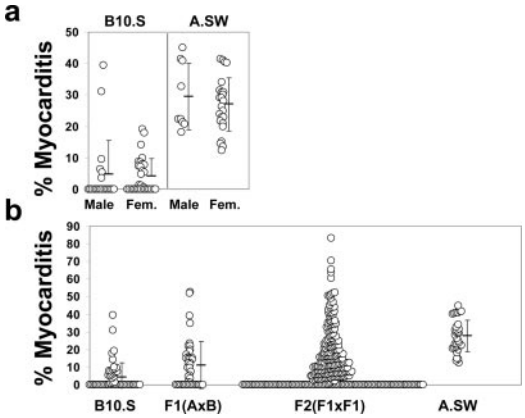

FIGURE 1. A.SW and B10.S mice demonstrate differences in autoimmune myocarditis. *A,* EAM was induced in 8- to 10-wk-old male and female A.SW and B10.S mice. Mice were immunized s.c. with murine cardiac myosin emulsified in CFA on days 0 and 7. The mice also received a single i.p. injection of pertussis toxin on day 0. After 3 wk, the mice were sacrificed, and the hearts were subjected to gross and microscopic examination. Examination of several cohorts of mice ($n = 4$–10 for each cohort, totaling $n = 51$ for B10.S, $n = 34$ for A.SW) subjected to the EAM protocol revealed a significant difference in the susceptibility of A.SW and B10.S mice. Percent area of myocardium affected by inflammation after induction of myocarditis for each individual is shown. Comparison of males and females within each strain shows no differences. In A.SW mice (male and female combined), 26.5 ± 9.2% of the myocardium is infiltrated by inflammation, whereas in B10.S mice, only 4.5 ± 7.5% of the myocardium is involved ($p = 1.6 \times 10^{-8}$). *B,* F_1 (A.SW × B10.S) (total $n = 44$) and F_2 ($F_1 \times F_1$) (total $n = 296$) crosses were performed to identify loci which control susceptibility to EAM. Percent area of myocardium affected by inflammation after induction of myocarditis for each individual is shown for A.SW, B10.S, F_1, and F_2 individuals.

mice, on average, 26.5 ± 9.2% of the myocardium was infiltrated by inflammation, whereas in B10.S mice, only 4.5 ± 7.5% of the myocardium was affected ($p = 1.6 \times 10^{-8}$) after induction of EAM. Comparison of male and female mice among the two strains showed no sex-based differences (Fig. 1*A*).

To determine whether susceptibility to EAM was a dominant trait, we tested several cohorts of F_1 (A.SW × B10.S) mice and found that susceptibility was intermediate and demonstrated substantial variability with 11.0 ± 13.4% of the myocardium infiltrated by chronic inflammatory cells after induction of EAM (Fig. 1*B*). This phenotype is significantly different from the phenotypes of both parents ($p = 6.8 \times 10^{-9}$ and 0.005 for comparisons of F_1 with A.SW and B10.S parents, respectively). The variation in the genetically homogenous parents, as well as in the F_1 strain, suggests substantial stochastic or environmental influence on susceptibility to EAM.

We next performed $F_1 \times F_1$ intercrosses to generate several cohorts of F_2 offspring and tested them by induction of EAM to identify loci that control susceptibility to disease by a standard Mendelian approach. F_2 offspring ($n = 296$) displayed a wide range of susceptibilities, but were heavily skewed toward the resistant phenotype (Fig. 1*B*).

Genetic crosses and linkage analysis reveal loci on Chr. 1 and 6 to be important in determining susceptibility to EAM

Because environmental factors seem to influence susceptibility to EAM, as displayed by the wide variation of parental A.SW, B10.S and especially F_1 mice, we decided to first analyze the extremes in phenotypes among F_2 animals for any linkage to chromosomal loci. F_2 offspring ($n = 144$) displaying susceptibility greater than or equal to the mean A.SW phenotype (percentage of myocarditis, >26.5) and less than or equal to the mean B10.S phenotype (percentage of myocarditis, <4.5) were selected. Thus the phenotype was simplified to a binary modality of either being susceptible or resistant. Genomic analysis was performed on these selected F_2 mice through determination of the inheritance pattern of A.SW and B10.S alleles of 81 SSLP markers spaced ~20 cM throughout the murine genome.

In the analysis of the 144 F_2 mice with extreme phenotypes, loci on Chr. 1 (LOD = 3.26; $p = 0.08$) and Chr. 6 (LOD = 3.26; $p = 0.06$) nearly reached the level of statistical significance (Fig. 2*A*). Loci on Chr. 4, 11, and 15 had LOD scores >2, but gave genome-wide p values of >0.25. Closer inspection of the strongest linkage, distal Chr. 6, revealed that there was a significant sex-related difference in inheritance of susceptibility. The locus on Chr. 6 appeared to affect only males. The LOD score for Chr. 6, for the analysis of the males only, was 4.99, with a genome-wide p value of 0.002 (Fig. 2*B*). The 1.5 LOD support interval, which may be viewed as an approximate 95% confidence interval for the quantitative trait linkage (QTL) location (26), covered ~10 cM at the telomere of Chr. 6.

Next, we wanted to determine whether inclusion of all 296 F_2 individuals in a QTL would provide additional evidence for the loci identified in the binary-trait analysis of 144 F_2 individuals with extreme phenotypes (presented above). All individuals were genotyped for loci on Chrs. 1, 4 and 6 with the addition of more SSLP markers. In the analysis of the QTL in all 296 F_2 mice, evidence for linkage was strongest for Chr. 6. The analysis of all mice gave a LOD score of 3.73 for Chr. 6 (genome-wide-adjusted $p = 0.01$; Fig. 3). The signal again came entirely from the male mice, with analysis in the male mice alone giving a LOD score of 5.70 (genome-wide-adjusted $p < 0.001$; Fig. 3*B*). The 1.5 LOD support interval covered ~9 cM. By this method, significant linkage was not observed for Chrs. 1 and 4. Controlling for the effect of the Chr. 6 locus did not reveal additional loci or affect the evidence for loci on Chrs. 1 and 4. No evidence for an interaction (epistasis) was observed.

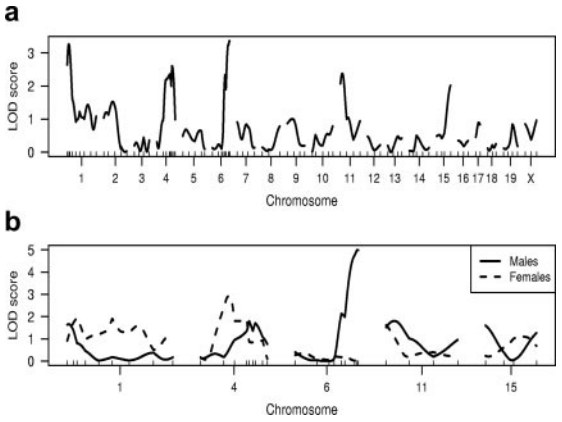

FIGURE 2. Genome-wide scan of F_2 individuals with extreme phenotypes reveals two possible loci on Chrs. 1 and 6 controlling susceptibility to EAM. *A,* F_2 offspring ($n = 144$) displaying susceptibility greater than or equal to the mean A.SW phenotype (percentage of myocarditis, >26.5) and less than or equal to the mean B10.S phenotype (percentage of myocarditis, <4.5) were selected for genomic analysis through determination of the inheritance pattern of A.SW and B10.S alleles of 81 SSLP markers distributed throughout the murine genome. The phenotype was treated as a binary trait—resistant or susceptible. LOD scores achieved at each of the 81 loci representing the entire murine genome are shown for each chromosome, ordered from centromere (*left*) to telomere (*right*). Linkage to loci on Chr. 1 (LOD = 3.26; $p = 0.08$) and Chr. 6 (LOD = 3.26; $p = 0.06$) were nearly statistically significant. Loci on Chr. 4, 11, and 15 had LOD scores >2, but gave genome-wide p values of >0.25. *B,* Closer inspection of the most significant linkage, distal Chr. 6, revealed that there was a significant gender difference in inheritance of susceptibility. LOD scores are displayed for each of the loci and determined separately for male and female mice. The locus on Chr. 6 appeared to have effect in only the males. Recalculation of the LOD score for Chr. 6, for the analysis of the males only, was 4.99, with a genome-wide p value of 0.002.

The A.SW allele at the Chr. 6 locus had the effect of increasing myocarditis, and was seen to be recessive to the B10.S allele. Only male individuals bearing the homozygous A.SW (AA) genotype at distal Chr. 6 exhibited susceptibility to EAM (Fig. 3*C*). Despite the significant influence of the A.SW Chr. 6 locus on disease susceptibility in males, 29% of male F_2 mice inheriting homozygous A.SW Chr. 6 alleles (AA) still exhibited intermediate susceptibility or resistance to autoimmune myocarditis similar to parental B10.S mice, suggesting that a combination of other loci (such as Chr. 1) and environmental factors influence susceptibility.

Thymocytes from A.SW mice demonstrate diminished susceptibility to Dxm-induced apoptosis

The NOD *Idd6* locus, which affects diabetes susceptibility, overlaps the A.SW EAM susceptibility locus on Chr. 6 identified here (22, 27, 28). In the NOD mouse, this locus has also been independently shown to modulate thymocyte susceptibility to Dxm-induced apoptosis, implicating defects in apoptotic pathways of autoreactive T cell precursors in the pathogenesis of diabetes (22, 29). After 12 h of Dxm treatment, female NOD thymocytes were shown to have a diminished degree of apoptosis compared with nondiabetic C57BL/6 controls (22, 29). We sought to determine whether A.SW thymocytes also demonstrate a similar phenotype because this locus is shared by two different strains demonstrating susceptibility to two different autoimmune diseases. In the original studies of NOD mice, information about male mice was not given.

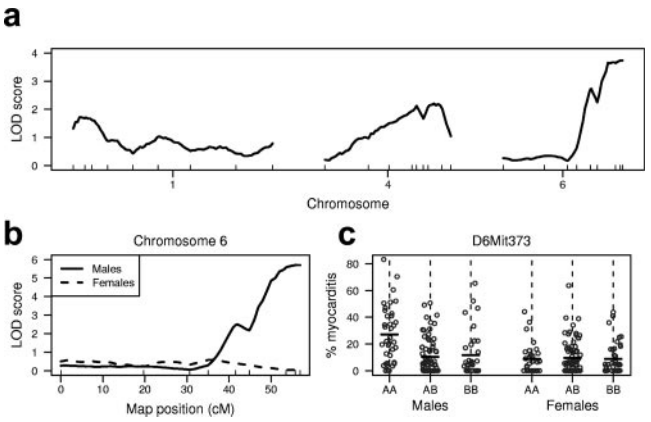

FIGURE 3. Quantitative trait analysis reveals strong linkage of Chr. 6 to susceptibility to EAM in male mice. *A,* LOD curves from the analysis of all 296 F_2 individuals with the phenotype treated as a quantitative trait are presented for Chrs. 1, 4, and 6. Only Chr. 6 reveals significant linkage with a LOD score of 3.73 (genome-wide-adjusted $p = 0.01$). *B,* Detail of Chr. 6 is shown for male and female mice separately. Analysis of male mice alone reveals a LOD score of 5.70 (genome-wide-adjusted $p < 0.001$). *C,* Phenotypes by sex and genotype at D6Mit373 are shown where AA represents homozygous A.SW, BB represents homozygous B10.S, and AB represents heterozygotes. Only male F_2 individuals homozygous for A.SW Chr. 6 alleles demonstrate increased susceptibility to EAM.

Because we identified sex-based differences in the effects of Chr. 6 in susceptibility to EAM, we compared Dxm-induced apoptosis in both male and female A.SW, B10.S, and NOD mice. Mice were challenged (i.p) with Dxm and thymocyte apoptosis was determined 12 h. later through TUNEL followed by flow cytometry. Consistent with the previous report (22, 29), thymocytes from female B10.S mice showed enhanced sensitivity to Dxm, demonstrating 29.5 ± 11.0% TUNEL-positive cells. In contrast, thymocytes from female A.SW mice, similar to female NOD mice, showed diminished susceptibility to Dxm, demonstrating 14.6 ± 10.5% and 14.4 ± 5.3% TUNEL-positive cells, respectively (p values for female B10.S-A.SW and B10.S-NOD comparisons are 1.3×10^{-5} and 1.2×10^{-5}, respectively). Interestingly, thymocytes from male B10.S, A.SW, and NOD mice showed similar susceptibility to Dxm-induced apoptosis, demonstrating 21.8 ± 15.0%, 24.1 ± 14.1%, and 25.9 ± 7.8% TUNEL-positive cells, respectively (Fig. 4). Thus there were significant sex-based differences in sensitivity to Dxm-induced thymocyte apoptosis in A.SW and NOD mice (p values for male A.SW-female A.SW and male NOD-female NOD comparisons are 0.006 and 0.001, respectively). Negative controls which included mice not treated with Dxm, and specificity controls, which included samples treated without TdT during the TUNEL reaction demonstrated <2.5% positivity (dUTP-FITC labeling).

Peripheral T cells from A.SW mice demonstrate diminished susceptibility to Cy-induced apoptosis

A second immunologic characteristic identified in NOD mice is the relative insensitivity of mature peripheral T lymphocytes to Cy-induced apoptosis compared with disease free C57BL/6 control mice (23). This trait, although similar to the thymic apoptosis trait described above, is associated with a different diabetes-susceptibility locus, *Idd5*, situated in the proximal portion of murine Chr. 1. This locus on Chr. 1 overlaps with the autoimmune myocarditis susceptibility locus identified here. Again, as reported in NOD mice, A.SW lymphocytes demonstrated diminished sensitivity to Cy-induced apoptosis as determined by TUNEL as described above. Lymphocytes from B10.S mice showed enhanced sensitivity to Cy: 45.5 ± 16.3% of B10.S lymphocytes whereas 22.9 ± 13.1% of A.SW lymphocytes were TUNEL positive after Cy treatment ($p = 1.23 \times 10^{-5}$) (Fig. 5). No sex-based differences were identified (data not shown).

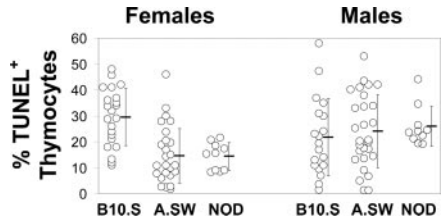

FIGURE 4. Similar to the diabetes-prone NOD mouse, A.SW thymocytes show diminished sensitivity to Dxm-induced apoptosis in a sex-specific manner. Male and female B10.S, A.SW, and NOD mice were treated with Dxm for 12 h (i.p.), and then the degree of thymocyte apoptosis was determined by TUNEL followed by FACS analysis. The combined results of four experiments are shown for both males and females. Thymocytes from female B10.S mice show enhanced sensitivity to Dxm, demonstrating 29.5 ± 11.0% TUNEL-positive cells. In contrast, thymocytes from female A.SW mice, similar to female NOD mice, show diminished susceptibility to Dxm, demonstrating 14.6 ± 10.5% and 14.4 ± 5.3% TUNEL-positive cells, respectively (p values for female B10.S-A.SW and B10.S-NOD comparisons are 1.3×10^{-5} and 1.2×10^{-5}, respectively). Thymocytes from male B10.S, A.SW, and NOD mice have similar susceptibility to Dxm-induced apoptosis, demonstrating 21.8 ± 15.0%, 24.1 ± 14.1%, and 25.9 ± 7.8% TUNEL-positive cells, respectively. Sex-based differences in sensitivity to Dxm-induced thymocyte apoptosis in A.SW and NOD mice are significant (p values for male A.SW-female A.SW and male NOD-female NOD comparisons are 0.006 and 0.001, respectively). Negative controls, which included mice not treated with Dxm, and specificity controls, which included samples treated without TdT during the TUNEL reaction, demonstrated <2.5% positivity.

Discussion

Susceptibility to EAM varies among different strains of mice and is influenced by both MHC and non-MHC genes (24, 25). However, unlike most models of autoimmune disease, non-MHC genes seem to have the greatest influence in EAM. For example, most A background mice such as A/J, A.SW, and A.CA, differing only at the MHC locus, develop severe myocarditis upon immunization with cardiac myosin, while most B strains of mice, such as C57BL/6J and C57BL/10J, are resistant to the induction of myocarditis. Therefore, it is an ideal system for the study of non-MHC

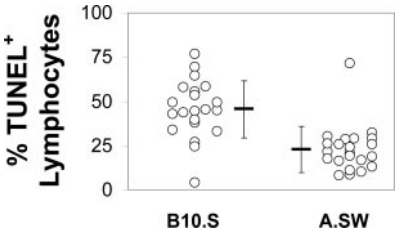

FIGURE 5. Similar to the diabetes-prone NOD mouse, A.SW lymphocytes show diminished sensitivity to Cy-induced apoptosis. Male and female B10.S and A.SW mice were treated with Cy for 12 h (i.p.), and then degree of lymphocyte apoptosis in lymph nodes was determined by TUNEL followed by FACS analysis. The combined results of three experiments are shown. A.SW lymphocytes demonstrated diminished sensitivity to Cy-induced apoptosis compared with B10.S lymphocytes: 45.5 ± 16.3% of B10.S lymphocytes whereas 22.9 ± 13.1% of A.SW lymphocytes were TUNEL positive after Cy treatment ($p = 1.23 \times 10^{-5}$). No sex-based differences were identified within each strain of mouse (data not shown).

genetic influences in autoimmune diseases. Thus MHC-congenic (H-2^s) strains were compared to identify non-MHC loci which influence disease.

In this study, we have identified a recessive locus on distal Chr. 6 to be strongly associated with susceptibility to EAM (LOD score of 5.70, $p < 0.001$), and will henceforth refer to this locus as *Eam2*. Uniquely, *Eam2* seems to be a susceptibility factor only in male mice, suggesting that the alleles in this locus require interaction with sex-specific factors to influence susceptibility to autoimmune myocarditis. Female mice inheriting the Chr. 6 susceptibility locus do not acquire disease. This is an unexpected finding especially when considering that the relative susceptibility to EAM among male and female A.SW mice and male and female B10.S mice is identical. This finding strongly suggests that additional genetic loci, such as Chr. 1 explained below, which must also operate in females, are involved in influencing susceptibility. Thus when all genetic loci are integrated, there is no overall sex-based difference.

In addition to Chr. 6, we have also identified a locus on Chr. 1 which is likely to influence susceptibility. Marked stochastic and environmental effects on disease were made evident by a wide range of susceptibilities, not only in F_1 heterozygous mice, but also to a lesser degree in parental A.SW and B10.S mice. We initially decided to study F_2 individuals with extremes in phenotypes, because these individuals are most likely to show minimal genetic heterogeneity. Through this approach which simplified the phenotype to either susceptible or resistant, highly suggestive linkage to proximal Chr. 1 (LOD score 3.26, $p = 0.08$) was identified in addition to the Chr. 6 locus. Like Chr. 6, this locus is recessive, but has effect in both male and female mice. A quantitative analysis which included all mice—intermediate susceptibility as well as extremes—failed to demonstrate significance at Chr. 1. This failure may be due to the confounding effects of intermediate susceptibility animals. These individuals are likely to have suboptimal combinations of susceptibility alleles and thus, they may be more influenced by uncontrolled environmental or stochastic factors compared with individuals which have multiple homozygous susceptibility alleles. For this reason, the genetic analysis of extremes of phenotypes may yield more accurate associations between loci and disease phenotypes, and suggest that at least proximal Chr. 1 is also a player in susceptibility to EAM. Further mapping studies will be needed to confirm the role of this locus.

Both the Chr. 1 and Chr. 6 loci (*Eam2*) identified here as influencing autoimmune myocarditis, have been previously identified in other autoimmune diseases. The NOD model of diabetes and murine experimental autoimmune orchitis both share proximal Chr. 1 as a susceptibility locus (28). The human counterpart of the proximal murine Chr. 1 locus has also been implicated in diabetes and autoimmune thyroid disease. The murine diabetes locus *Idd6* on distal Chr. 6 overlaps with *Eam2*. This strongly suggests that that there are common mechanisms leading to autoimmune diseases, with other genetic and environmental influences determining tissue specificity of disease. Indeed, a recent survey of published linkage studies on autoimmune or immune-mediated diseases revealed several overlapping syntenic human and mouse chromosomal regions with a cluster of disease susceptibility loci (28). These studies provide support for the concept that autoimmune disorders in different species are controlled by a common set of susceptibility genes. Therefore, understanding the mechanisms that lead to the disease in animals may provide fresh insight into their human disease counterparts.

One of the next phases in autoimmunity research, stemming from mapping studies, will be the molecular identification of susceptibility alleles. Located in the proximal Chr. 1 locus identified here, CTLA-4 is an immunologically important regulatory molecule that has been implicated in several autoimmune diseases like autoimmune thyroid disease and in the murine model of type-1 diabetes, NOD (30, 31). Recently, it has been shown that polymorphisms within CTLA-4 genomic sequences influencing alternative splicing of CTLA-4 is most likely cause of linkage to this locus in human autoimmune thyroid disease and murine diabetes (32). It is currently not known how changes in the relative expression of these splice forms influences autoimmune disease, but it is thought that these particular alterations in the expression of CTLA-4 isoforms can diminish the total inhibitory signal that is delivered to activated self-reactive T cells, thus increasing the likelihood of autoimmunity. Consistent with this hypothesis, we have found that treatment with mAb to CTLA-4 intensifies EAM in moderately susceptible BALB/c mice and even renders resistant C57BL/6 mice susceptible (D. Cihakova and N. Rose, unpublished data).

Due to the overlapping autoimmune susceptibility loci in A.SW and NOD mice, we were interested to determine whether EAM-susceptible A.SW and diabetes-susceptible NOD mice shared phenotypic characteristics that may render both strains susceptible to autoimmune disorders. In addition to developing spontaneous diabetes, NOD mice display a multitude of immunologic peculiarities. For example, immature T cells in the thymus of female NOD mice are relatively insensitive to induction of apoptosis by the stressor, Dxm, compared with disease-free control mice (22, 33). Decreased potential for apoptosis in NOD thymocytes could potentially lead to retention of autoreactive T cells and susceptibility to an autoimmune disease like diabetes. Interestingly, this trait, differential sensitivity to Dxm-induced apoptosis, was independently mapped to the distal portion of murine Chr. 6—the same locus that already harbors a diabetes susceptibility locus, *Idd6,* and now, *Eam2*, the locus identified here as influencing susceptibility to autoimmune myocarditis (29). Due to the colocalization of autoimmune susceptibility and apoptosis-sensitivity in NOD mice, we asked whether A.SW mice, which are susceptible to EAM, also demonstrate diminished susceptibility to Dxm-induced thymocyte apoptosis. Indeed, like in NOD mice, A.SW thymocytes demonstrated diminished sensitivity to apoptosis compared with the autoimmune myocarditis resistant strain B10.S.

Recent NOD congenic lines have confirmed the role of *Idd6* on Chr. 6 as a player in susceptibility to diabetes in the NOD mouse (22). Interestingly, it was discovered that this locus had a greater influence in male mice compared with females, paralleling our finding of the exclusive role of *Eam2* in male mice. These two independent observations suggest that this autoimmunity locus interacts with sex-specific factors in influencing susceptibility to autoimmune disease. Furthermore, this locus imparts differential thymocyte apoptosis in a sex-specific manner, where only female mice demonstrate phenotypic differences among the strains analyzed. Further investigation is needed to understand the discrepancy in the sex-based effect of this locus where differential susceptibility to autoimmune disease is apparent in males whereas differential susceptibility to Dxm-induced thymocyte apoptosis is only in females. It is not known whether the polymorphic genes responsible for differential susceptibility to autoimmune disease (diabetes in NOD, and EAM in A.SW) and differential sensitivity to apoptosis are identical, or just tightly linked. Discrepancy in the sex-bias between these two phenotypes could suggest that they are controlled by tightly linked but separate genes. Accordingly, this specific chromosomal location may be influenced in a gender-specific manner, imparting the effect on a multitude of genes in the region. Alternatively, the mere presence of a significant sex-based influence on both genetically linked phenotypes, autoimmunity

and apoptosis, could also suggest that there is a single gene controlling both phenotypes. According to this hypothesis, this gene would manifest opposite gender-bias depending on the phenotype analyzed. Finer mapping which may reveal two separate loci, or finally, identification of responsible polymorphisms controlling the two phenotypes will ultimately resolve this discrepancy in sex-bias.

A second immunologic feature of NOD mice is the relative insensitivity of mature peripheral T lymphocytes to Cy-induced apoptosis compared with disease free control mice (23). This trait, although similar to the thymic apoptosis trait described above, has been independently mapped in the NOD mouse, to the proximal portion of murine Chr. 1. This is the same area on Chr. 1 that is shared by the diabetes susceptibility locus, *Idd5*, and the autoimmune myocarditis susceptibility locus identified here with highly suggestive linkage. Due to this association, we asked whether A.SW mice demonstrated a phenotype similar to NOD mice. Again, like in NOD mice, A.SW lymphocytes demonstrated diminished sensitivity to Cy-induced apoptosis. Although the establishment of proximal Chr. 1 as a bona fide EAM susceptibility locus will require additional work, the highly suggestive linkage achieved with this study combined with the observation that A.SW and NOD mice share a similar apoptosis phenotype which has been firmly linked to this locus in NOD mice strengthens the evidence that Chr. 1 is an important player in susceptibility to autoimmune myocarditis.

In summary, NOD mice that spontaneously develop diabetes and A.SW mice which are susceptible to EAM not only share two susceptibility loci, but also demonstrate two functional abnormalities associated with apoptosis of T cells. These two loci affect apoptosis at different stages of T cell development: Chr. 6 influences immature thymocyte apoptosis and Chr. 1 affects apoptosis in mature peripheral T cells. Further work is required to establish that the genetic elements which control sensitivity to drug-induced apoptosis at either of these loci are the same genetic elements that control susceptibility to autoimmune disease. Finally, it will be important to determine how polymorphisms at these loci influence apoptosis and whether they control susceptibility to different autoimmune diseases.

Acknowledgments

We thank Dr. Patrizio Caturegli for helpful discussions and review of the manuscript

References

1. Brown, C. A., and J. B. O'Connell. 1995. Myocarditis and idiopathic dilated cardiomyopathy. *Am. J. Med. 99:309*.
2. Drory, Y., Y. Turetz, Y. Hiss, B. Lev, E. Z. Fisman, A. Pines, and M. R. Kramer. 1991. Sudden unexpected death in persons less than 40 years of age. *Am. J. Cardiol. 68:1388*.
3. Felker, G. M., W. Hu, J. M. Hare, R. H. Hruban, K. L. Baughman, and E. K. Kasper. 1999. The spectrum of dilated cardiomyopathy: The Johns Hopkins experience with 1,278 patients. *Medicine 78:270*.
4. Rose, N. R., A. Herskowitz, D. A. Neumann, and N. Neu. 1988. Autoimmune myocarditis: a paradigm of post-infection autoimmune disease. *Immunol. Today 9:117*.
5. Rose, N. R., L. J. Wolfgram, A. Herskowitz, and K. W. Beisel. 1986. Postinfectious autoimmunity: two distinct phases of coxsackievirus B3-induced myocarditis. *Ann. NY Acad. Sci. 475:146*.
6. Caforio, A. L., J. H. Goldman, A. J. Haven, K. M. Baig, L. D. Libera, and W. J. McKenna. 1997. Circulating cardiac-specific autoantibodies as markers of autoimmunity in clinical and biopsy-proven myocarditis: The Myocarditis Treatment Trial Investigators. *Eur. Heart J. 18:270*.
7. Caforio, A. L., J. H. Goldman, A. J. Haven, K. M. Baig, and W. J. McKenna. 1996. Evidence for autoimmunity to myosin and other heart-specific autoantigens in patients with dilated cardiomyopathy and their relatives. *Int. J. Cardiol. 54:157*.
8. Wolfgram, L. J., K. W. Beisel, and N. R. Rose. 1985. Heart-specific autoantibodies following murine coxsackievirus B3 myocarditis. *J. Exp. Med. 161:1112*.
9. Neu, N., K. W. Beisel, M. D. Traystman, N. R. Rose, and S. W. Craig. 1987. Autoantibodies specific for the cardiac myosin isoform are found in mice susceptible to coxsackievirus B3-induced myocarditis. *J. Immunol. 138:2488*.
10. Neu, N., N. R. Rose, K. W. Beisel, A. Herskowitz, G. Gurri Glass, and S. W. Craig. 1987. Cardiac myosin induces myocarditis in genetically predisposed mice. *J. Immunol. 139:3630*.
11. Smith, S. C., and P. M. Allen. 1991. Myosin-induced acute myocarditis is a T cell-mediated disease. *J. Immunol. 147:2141*.
12. Smith, S. C., and P. M. Allen. 1993. The role of T cells in myosin-induced autoimmune myocarditis. *Clin. Immunol. Immunopathol. 68:100*.
13. Wolfgram, L. J., K. W. Beisel, A. Herskowitz, and N. R. Rose. 1986. Variations in the susceptibility to coxsackievirus B3-induced myocarditis among different strains of mice. *J. Immunol. 136:1846*.
14. Traystman, M. D., and K. W. Beisel. 1991. Genetic control of coxsackievirus B3-induced heart-specific autoantibodies associated with chronic myocarditis. *Clin. Exp. Immunol. 86:291*.
15. Neu, N., S. W. Craig, N. R. Rose, F. Alvarez, and K. W. Beisel. 1987. Coxsackievirus induced myocarditis in mice: cardiac myosin autoantibodies do not cross-react with the virus. *Clin. Exp. Immunol. 69:566*.
16. Gorham, J. D., M. L. Guler, R. G. Steen, A. J. Mackey, M. J. Daly, K. Frederick, W. F. Dietrich, and K. M. Murphy. 1996. Genetic mapping of a murine locus controlling development of T helper 1/T helper 2 type responses. *Proc. Natl. Acad. Sci. USA 93:12467*.
17. Broman, K. W., H. Wu, S. Sen, and G. A. Churchill. 2003. R/qtl: QTL mapping in experimental crosses. *Bioinformatics 19:889*.
18. Ihaka, R., and R. Gentleman. 1996. R: a language for data analysis and graphics. *J. Comput. Graph. Stat. 5:299*.
19. Xu, S., and W. R. Atchley. 1996. Mapping quantitative trait loci for complex binary diseases using line crosses. *Genetics 143:1417*.
20. Churchill, G. A., and R. W. Doerge. 1994. Empirical threshold values for quantitative trait mapping. *Genetics 138:963*.
21. Sen, S., and G. A. Churchill. 2001. A statistical framework for quantitative trait mapping. *Genetics 159:371*.
22. Bergman, M. L., N. Duarte, S. Campino, M. Lundholm, V. Motta, K. Lejon, C. Penha-Goncalves, and D. Holmberg. 2003. Diabetes protection and restoration of thymocyte apoptosis in NOD Idd6 congenic strains. *Diabetes 52:1677*.
23. Colucci, F., M. L. Bergman, C. Penha-Goncalves, C. M. Cilio, and D. Holmberg. 1997. Apoptosis resistance of nonobese diabetic peripheral lymphocytes linked to the Idd5 diabetes susceptibility region. *Proc. Natl. Acad. Sci. USA 94:8670*.
24. Rose, N. R., D. A. Neumann, A. Herskowitz, M. D. Traystman, and K. W. Beisel. 1988. Genetics of susceptibility to viral myocarditis in mice. *Pathol. Immunopathol. Res. 7:266*.
25. Beisel, K. W., L. Wolfgram, A. Hershkowitz, and N. R. Rose. 1985. Differences in severity of coxsackievirus B3-induced myocarditis among H-2 congenic strains. In *Genetic Control of Host Resistance to Infection and Malignancy*. E. Skamane, ed. Liss, New York, p. 195.
26. Dupuis, J., and D. Siegmund. 1999. Statistical methods for mapping quantitative trait loci from a dense set of markers. *Genetics 151:373*.
27. Wicker, L. S., J. A. Todd, and L. B. Peterson. 1995. Genetic control of autoimmune diabetes in the NOD mouse. *Annu. Rev. Immunol. 13:179*.
28. Vyse, T. J., and J. A. Todd. 1996. Genetic analysis of autoimmune disease. *Cell 85:311*.
29. Penha-Goncalves, C., K. Leijon, L. Persson, and D. Holmberg. 1995. Type 1 diabetes and the control of dexamethazone-induced apoptosis in mice maps to the same region on chromosome 6. *Genomics 28:398*.
30. Chang, T. T., V. K. Kuchroo, and A. H. Sharpe. 2002. Role of the B7-CD28/CTLA-4 pathway in autoimmune disease. *Curr. Dir. Autoimmun. 5:113*.
31. Kristiansen, O. P., Z. M. Larsen, and F. Pociot. 2000. CTLA-4 in autoimmune diseases—a general susceptibility gene to autoimmunity? *Genes Immun. 1:170*.
32. Ueda, H., J. M. Howson, L. Esposito, J. Heward, H. Snook, G. Chamberlain, D. B. Rainbow, K. M. Hunter, A. N. Smith, G. Di Genova, et al. 2003. Association of the T-cell regulatory gene CTLA4 with susceptibility to autoimmune disease. *Nature 423:506*.
33. Bergman, M. L., C. Penha-Goncalves, K. Lejon, and D. Holmberg. 2001. Low rate of proliferation in immature thymocytes of the non-obese diabetic mouse maps to the Idd6 diabetes susceptibility region. *Diabetologia 44:1054*.